

EXPERIMENTAL RESULTS OF WINGLETS

ON FIRST, SECOND, AND THIRD

GENERATION JET TRANSPORTS

Stuart G. Flechner and Peter F. Jacobs

NASA Langley Research Center

SUMMARY

Winglets are intended to provide substantially greater reductions in drag coefficient, at cruise conditions, than those obtained with a simple wing-tip extension. Extensive experimental investigations have been conducted by NASA to show the effect of winglets on jet transports. This paper presents the results of wind-tunnel investigations of four jet transport configurations representing both narrow and wide-body configurations and also a future advanced aerodynamic configuration. Performance and wing-root bending moment data are presented. In support of a winglet flight research and demonstration program, a comprehensive wind-tunnel investigation was undertaken on one transport configuration to determine the effects of winglets on the aerodynamic characteristics throughout the flight envelope. The investigation was designed to identify any adverse effects due to winglets.

The results of the investigations indicate that winglets improved the cruise lift-to-drag ratio between 4 and 8 percent, depending on the transport configuration. The data also indicate that ratios of relative aerodynamic gain to relative structural weight penalty for winglets are 1.5 to 2.5 times those for wing-tip extensions. The comprehensive investigation has indicated that, over the complete range of flight conditions, winglets produce no adverse effects on buffet onset, lateral-directional stability, and aileron control effectiveness. A winglet flight research and demonstration program has been initiated and results are expected to be available near the end of 1979.

INTRODUCTION

The National Aeronautics and Space Administration has been conducting extensive experimental investigations of the effects of winglets on jet transports. (See refs. 1 to 8.) Winglets, described in detail in reference 1, are intended to provide reductions in drag coefficient, at cruise conditions, substantially greater than those obtained with a simple wing-tip extension.

This paper presents the results of wind-tunnel investigations in the Langley 8-foot transonic pressure tunnel of winglets on four jet transport configurations. Performance and wing-root bending moment data are given for these configurations which represent three generations of jet transports; narrow bodies, wide bodies, and a future advanced aerodynamic concept. In

addition, for one configuration, detailed aerodynamic characteristics are presented at the design condition and also at several off-design conditions. Finally, some milestones in the joint USAF/NASA Winglet Flight Research and Demonstration Program will be presented.

SYMBOLS

The results presented are referred to the stability-axis system for the longitudinal aerodynamic characteristics and to the body-axis system for the lateral-directional aerodynamic characteristics. Force and moment data have been reduced to conventional coefficient form based on the geometry of the basic wing planform for each transport configuration. All measurements and calculations were made in U.S. Customary Units.

AR	aspect ratio
b	wing span
C_B	wing-root bending-moment coefficient, $\frac{\text{Bending moment}}{q_\infty (S/2)(b/2)}$
C_L	lift coefficient, $\frac{\text{Lift}}{q_\infty S}$
C_{l_β}	rate of change of rolling-moment coefficient with sideslip angle (effective dihedral parameter)
$C_{l_{\delta_a}}$	rate of change of rolling-moment coefficient with differential aileron deflection (aileron control effectiveness)
C_n	section normal-force coefficient obtained from integration of pressure measurements
C_{n_β}	rate of change of yawing-moment coefficient with sideslip angle (directional stability parameter)
c	local chord
\bar{c}	mean aerodynamic chord of basic configuration
h	span of the upper winglet, measured from the wing chord plane
L/D	lift-to-drag ratio
M_∞	free-stream Mach number
q_∞	free-stream dynamic pressure

R	ratio of merit
S	basic configuration wing planform reference area
SCW	supercritical wing
y	spanwise distance from wing-fuselage juncture, positive outboard
z'	distance along winglet span from chord plane of wing
α	angle of attack
β	angle of sideslip
Δ	incremental value
$\delta_{a,L}; \delta_{a,R}$	left and right aileron deflection, positive for trailing edge down
δ_f	flap deflection, positive for trailing edge down
δ_h	horizontal-tail deflection, positive for trailing edge down
Subscripts:	
BASIC	reference configuration, model with no wing-tip devices
CRUISE	condition at cruise C_L or cruise M_∞ or both
MAX	condition at maximum bending moment

FUNCTION OF WINGLET

Winglets are small, nearly vertical aerodynamic surfaces which are designed to be mounted at the tips of aircraft wings. (See fig. 1.) Unlike flat end plates, winglets are designed with the same careful attention to airfoil shape and local flow conditions as the wing itself. The primary component of the winglet configurations is a large winglet mounted rearward above the wing tip. The "upper surface" of this airfoil is the inboard surface. For some configurations an additional small winglet, mounted forward, below the wing tip, is necessary. The "upper surface" of the airfoil for this lower winglet is the outboard surface.

The winglets operate in the circulation field around the wing tip. Because of the pressure differential between the wing surfaces at the tip, the air flow tends to move outboard along the wing lower surface, around the tip, and inboard along the wing upper surface. This wing-tip vortex produces cross flows at each winglet. Thus the winglets produce large side forces even at low aircraft angles of attack. Since the side force vectors are

approximately perpendicular to the local flow, the side forces produced by the winglets have forward (thrust) components (fig. 1) which reduce the aircraft induced drag. This is the same principle that enables a sailboat to travel upwind by tacking. For winglets to be fully effective the side forces must be produced as efficiently as possible; therefore, advanced aerodynamic airfoil shapes are used. The side force produced by the winglets, and therefore the thrust produced, is dependent upon the strength of the circulation around the wing tip. Since the circulation strength is a function of the lift loads near the wing tip, winglets are more effective on those aircraft with higher wing loads near the tip.

Theoretical calculations indicate that the aerodynamic benefit would be the same for a given size winglet in either the upper or lower position. Ground clearance of low-wing jet transports limits the span of the lower winglet, and interference with the upper winglet flow limits the chord length of the lower winglet. Thus, from a practical standpoint for low-wing aircraft the lower winglet must be relatively small. As a result, for the jet transports being discussed herein, the contributions of the lower winglet to the reduction of drag were relatively small.

As indicated on figure 1, the winglets tend to straighten the air flow thus slightly reducing the wing-tip vortex strength. However, the trailing vortex hazard still exists. The reduction is an indication of an increase in the aircraft efficiency. Winglets are not designed to improve flight safety for trailing aircraft, but to increase aerodynamic efficiency.

WINGLET EFFECTIVENESS

Configurations

As previously indicated, four jet transport configurations were investigated in the Langley 8-foot transonic pressure tunnel. Photographs of the models are presented in figure 2. First generation jet transports, those with narrow bodies, are represented by the KC-135A. Second generation jet transports, those with wide bodies, are represented by the L-1011 and the DC-10. The third or future generation of jet transports, those with wide bodies and advanced aerodynamic concepts, are represented by a high-aspect-ratio supercritical wing model. This is the "current" (9.8-AR) configuration of reference 9.

Semispan models of the KC-135A and the DC-10 enabled those investigations to be conducted at increased Reynolds numbers, approximately 7 and 5 million, based on mean geometric chords, respectively. Forces and moments were measured by a strain gage balance. The KC-135A fuselage was not attached to the balance but the DC-10 fuselage was attached. The fuselages for the full-span L-1011 and high-aspect-ratio supercritical wing models were represented by bodies of revolution.

The KC-135A and the high-aspect-ratio supercritical wing models did not utilize lower surface winglets. The L-1011 and the DC-10 did utilize the lower surface winglets.

Performance

Figure 3 presents the aerodynamic gain due to winglets for each configuration at its cruise lift coefficient. The aerodynamic gain is represented by the percentage increase in lift-to-drag ratio (L/D) over the basic configurations. At the cruise Mach numbers, indicated by tick marks on the figure, the winglets produced about an 8 percent improvement in L/D for the KC-135A, about a 4 percent improvement for both the L-1011 and DC-10, and about a 6.5 percent improvement for the high-aspect-ratio configuration. Analysis of the data indicated that the KC-135A winglets achieved the greatest performance improvement because the KC-135A has the highest outboard wing loading of those configurations investigated. The KC-135A has an elliptical spanwise load distribution. One characteristic of wide body transports is wing loads over the outboard wing region less than those of an elliptic distribution. This is reflected in reduced winglet performance improvements on the L-1011 and the DC-10. The high-aspect-ratio model was designed for nearly an elliptical spanwise load distribution and therefore the aerodynamic gains with winglets are high, approaching the gains of the KC-135A with winglets. The data shown have not been corrected for full-scale Reynolds number. This correction would result in approximately a one percent increase in lift-to-drag ratio.

It was suggested that the same aerodynamic gains could be obtained simply by increasing the wing span, that is, by adding a wing-tip extension. Therefore as part of each investigation a simple wing-tip extension configuration was also tested. The wing-tip extension for the KC-135A was designed to have the same increase in wing-root bending moment as that due to the winglet at the cruise lift coefficient. This resulted in an increase in the semispan which was equal to 38 percent of the winglet span.

The tip extension configuration for the L-1011 represented a configuration under consideration by the aircraft company. The increase in semispan was approximately 40 percent of the upper winglet span. The DC-10 tip extension represents the change from the Series 10 wing to the Series 30 wing. (The winglet was tested on the Series 10 wing.) The increase in semispan was about 47 percent of the upper winglet span.

The tip extension configuration for the high-aspect-ratio supercritical wing configuration was represented by a higher aspect ratio (11.4) model of reference 9. The increase in semispan was equal to the winglet span.

Figure 3 also presents the aerodynamic gains at cruise lift coefficient for tip extensions. Tip extension performance gains at cruise Mach numbers were about 4 percent for the KC-135A, about 2.5 percent for the L-1011 and the DC-10, and about 7 percent for the high-aspect-ratio supercritical wing configuration. Again, loading near the wing tip affects the gains achieved, but direct comparisons cannot be made because of the different wing-tip extension sizes.

Wing-Root Bending Moments

In the structural design of wings the spanwise variation in bending moments must be considered. Unpublished analysis of wing structures has indicated that structural weight changes are roughly proportional to changes in the wing-root bending moments. Therefore, increases in the maximum wing-root bending moment will be used to approximate structural weight penalties.

Figure 4 presents the percentage increase in wing-root bending moment with winglets or tip extensions over the basic configuration at the maximum wing-root bending moment condition. For uniformity in presenting the data, the maximum wing-root bending moment was considered to occur at the lift coefficient where the plot of pitching-moment coefficient versus lift coefficient becomes nonlinear. The data show that the incremental increase in maximum wing-root bending moment due to tip extensions is always equal to or greater than the incremental increase due to winglets.

The bending moment increments for the KC-135A are lower than those for the other configurations because the KC-135A model wing was designed to aeroelastically deflect the same as the aircraft wing. The other models were rigid representatives of the cruise shape. The aeroelastic deflection reduces the added moments due to the winglets and thus reduces the maximum wing-root bending moment condition.

Relative Merits

To compare the four jet transport configurations with winglets and tip extensions the aerodynamic gain and the structural weight penalty have been considered together in a new term. For this comparison the term ratio of merit has been employed and is defined as the relative aerodynamic gain at cruise lift coefficient, represented by the percentage increase in lift-to-drag ratio over the basic configuration (fig. 3), divided by the relative structural weight penalty at the maximum wing-root bending moment condition, approximated by the percentage increase in wing-root bending moment over the basic configuration (fig. 4). That is,

$$R \approx \frac{\left(\frac{\Delta L/D}{(L/D)_{\text{BASIC}}} \right)_{\text{CRUISE}}}{\left(\frac{\Delta C_B}{C_{B, \text{BASIC}}} \right)_{\text{MAX}}}$$

The comparison of the ratios of merit is present in figure 5. As defined by this parameter, winglets are more effective than wing-tip extensions for all the jet transport configurations investigated. (Note the change in scale for the L-1011 and DC-10.) At the cruise Mach number, winglets on the KC-135A provided 2.5 times the improvement of the tip extension in ratio of merit. The winglets on the L-1011 and DC-10 provided improvements at the cruise Mach numbers 1.5 and 2 times those of the tip extensions, respectively. The

winglets on the high-aspect-ratio supercritical wing provided improvement at the cruise Mach number 2 times those of the tip extension.

The ratio of merit for the KC-135A with winglets is greater for two reasons. First, the KC-135A has the highest loading over the outboard wing region resulting in the largest aerodynamic gains from winglets. Secondly, the aeroelastic wing reduced the maximum wing-root bending moments. Aeroelastic wing deflection for the other jet transport models would increase the relative gains for winglets over tip extensions as expressed by the ratio of merit.

DETAILED INVESTIGATIONS

After the benefits obtainable with winglets first became known the U. S. Air Force initiated design studies on the application of the winglet concept, references 10 and 11. (Winglets were also known as vortex diffusers and tip fins.) The potential large fuel savings available by retrofitting winglets to the USAF fleet of large transports has led to a joint USAF/NASA Winglet Flight Research and Demonstration Program. The KC-135A was chosen as the test bed aircraft. Aerodynamically, the KC-135A is an ideal test bed. As previously indicated, the ratios of merit are very high.

In support of this flight program, a comprehensive wind-tunnel investigation was undertaken to determine the aerodynamic characteristics of the KC-135A with winglets throughout the flight envelope. Specifically, the investigation was designed to identify any adverse effects due to winglets. While the results of the investigation are for the KC-135A, the trends indicated are judged to be valid for most large jet transports with winglets.

Wind-Tunnel Models

The comprehensive investigation required four different wind-tunnel model configurations as shown in figure 6. As previously indicated, the semispan model was used to obtain all performance and some loads data. A full-span model with changeable flaps and ailerons was used to obtain the low-speed ($M_{\infty} = 0.30$) stability and control characteristics. The same fuselage and tail with a pressure instrumented wing was used to obtain high-speed stability and loads data in yaw. The pressure instrumented wing on a tailless body of revolution fuselage was used to obtain stability and loads data at high angles of attack.

Low-Speed Performance

The aerodynamic gain due to winglets at 0.30 Mach number and in a take-off configuration is presented in figure 7. Again, the aerodynamic gain is represented by the percentage increase in lift-to-drag ratio over the basic configuration. The lift coefficient range of interest for low speed performance is substantially higher than the lift coefficient for cruise performance. At these higher lift coefficients the induced drag is a higher percent of the total drag than at the cruise lift coefficient. Since the higher induced drag

indicates the circulation around the wing tip is stronger, the winglet effectiveness is also increased.

Spanwise Load Distribution

Figure 8 presents the effects due to winglets on the spanwise load distribution of the KC-135A and the load distribution along the winglet span. Two lift coefficients, representing the maximum wing-root bending moment condition and the cruise condition, are shown at the cruise Mach number, 0.78. The elliptical spanwise load distribution of the basic KC-135A is shown along with the increase in load near the tip due to the winglet. The effect of the aeroelastic deflection is also shown by the fact that the relative increase in load near the tip due to the winglets is smaller at the high lift coefficient than the increase at the cruise lift coefficient.

Buffet Characteristics

The effect of winglets on the KC-135A buffet characteristics is shown on figure 9. Buffet was considered to occur at the lift coefficient of the initial break in the plot of lift coefficient versus angle of attack. Below the cruise Mach number the lift coefficient for buffet onset is generally higher with winglets on. Above the cruise Mach number there is no significant change in the buffet characteristics.

Lateral-Directional Stability

The effects of winglets on the KC-135A lateral-directional stability is presented in figure 10(a) for high-speed conditions and in figure 10(b) for low-speed conditions. At cruise lift coefficient, winglets increase the high-speed effective dihedral between 10 and 19 percent and increase the directional stability approximately 9 percent. The data presented at the low-speed condition is for a configuration with take-off flaps and moderate differential aileron deflection. Again winglets increase the effective dihedral between 7 and 24 percent and increase the directional stability between 3 and 16 percent. Similar trends were obtained for landing flap conditions and for aileron deflections of 0° and 20° .

Aileron Control Effectiveness

Figure 11 presents the effects of winglets on KC-135A low speed aileron control effectiveness. The data presented in figure 11 is again for the configuration with take-off flaps. The winglets increase the aileron control effectiveness between 3 and 13 percent. Similar trends were also obtained for the landing flap configuration.

FLIGHT RESEARCH AND DEMONSTRATION PROGRAM

As previously mentioned NASA and the USAF are conducting a joint Winglet Flight Research and Demonstration Program using the KC-135A aircraft. An artist's concept of the configuration is shown in figure 12. Final structural

design of the flight hardware is underway. The base-line documentation flights are scheduled to begin during August 1978. The first flight with winglets is anticipated in early 1979 and the flight-test data will be available in the fall of 1979, about three months after the last flight.

SUMMARY OF RESULTS

Wind-tunnel investigations of winglets and tip extensions on model configurations representing three generations of jet transports have been conducted. The data presented indicate the following conclusions:

1. Winglets improved the cruise lift-to-drag ratio between 4 and 8 percent, depending upon the configuration and, in particular, the span load distribution.

2. The ratio of relative aerodynamic gain to relative structural weight penalty for winglets are 1.5 to 2.5 times the ratio for wing-tip extensions.

3. A comprehensive wind-tunnel investigation of winglets on the USAF KC-135A over the complete range of flight conditions has indicated that winglets produce no adverse effects on buffet onset, lateral-directional stability, or aileron control effectiveness.

4. A Winglet Flight Research and Demonstration Program is under way utilizing the KC-135A as the test vehicle. The flight-test results will be available near the end of 1979.

REFERENCES

1. Whitcomb, Richard T.: A Design Approach and Selected Wind-Tunnel Results at High Subsonic Speeds for Wing-Tip Mounted Winglets. NASA TN D-8260, 1976.
2. Flechner, Stuart G.; Jacobs, Peter F.; and Whitcomb, Richard T.: A High Subsonic Speed Wind-Tunnel Investigation of Winglets on a Representative Second-Generation Jet Transport Wing. NASA TN D-8264, 1976.
3. Jacobs, Peter F.; and Flechner, Stuart G.: The Effect of Winglets on the Static Aerodynamic Stability Characteristics of a Representative Second Generation Jet Transport Model. NASA TN D-8267, 1976.
4. Jacobs, Peter F.; Flechner, Stuart G.; and Montoya, Lawrence C.: Effect of Winglets on a First-Generation Jet Transport Wing. I - Longitudinal Aerodynamic Characteristics of a Semispan Model at Subsonic Speeds. NASA TN D-8473, 1977.
5. Montoya, Lawrence C.; Flechner, Stuart G.; and Jacobs, Peter F.: Effect of Winglets on a First-Generation Jet Transport Wing. II - Pressure and Spanwise Load Distributions for a Semispan Model at High Subsonic Speeds. NASA TN D-8474, 1977.
6. Montoya, Lawrence C.; Jacobs, Peter F.; and Flechner, Stuart G.: Effect of Winglets on a First-Generation Jet Transport Wing. III - Pressure and Spanwise Load Distributions for a Semispan Model at Mach 0.30. NASA TN D-8478, 1977.
7. Meyer, Robert R., Jr.: Effect of Winglets on a First-Generation Jet Transport Wing. IV - Stability Characteristics for a Full-Span Model at Mach 0.30. NASA TP-1119, 1978.
8. Jacobs, Peter F.: Effect of Winglets on a First-Generation Jet Transport Wing. V - Stability Characteristics of a Full-Span Wing With a Generalized Fuselage at High Subsonic Speeds. NASA TP-1163, 1978.
9. Bartlett, Dennis W.; and Patterson, James C., Jr.: NASA Supercritical-Wing Technology. NASA TM-78731, 1978.
10. Kulfan, Robert M.; and Howard, Weston M.: Application of Advanced Aerodynamic Concepts to Large Subsonic Transport Airplanes. AFFDL-TR-75-112, U.S. Air Force, Nov. 1975.
11. Ishimitsu, K. K.; VanDevender, N.; Dodson, R.; et al.: Design and Analysis of Winglets for Military Aircraft. AFFDL-TR-76-6, U.S. Air Force, Feb. 1976.

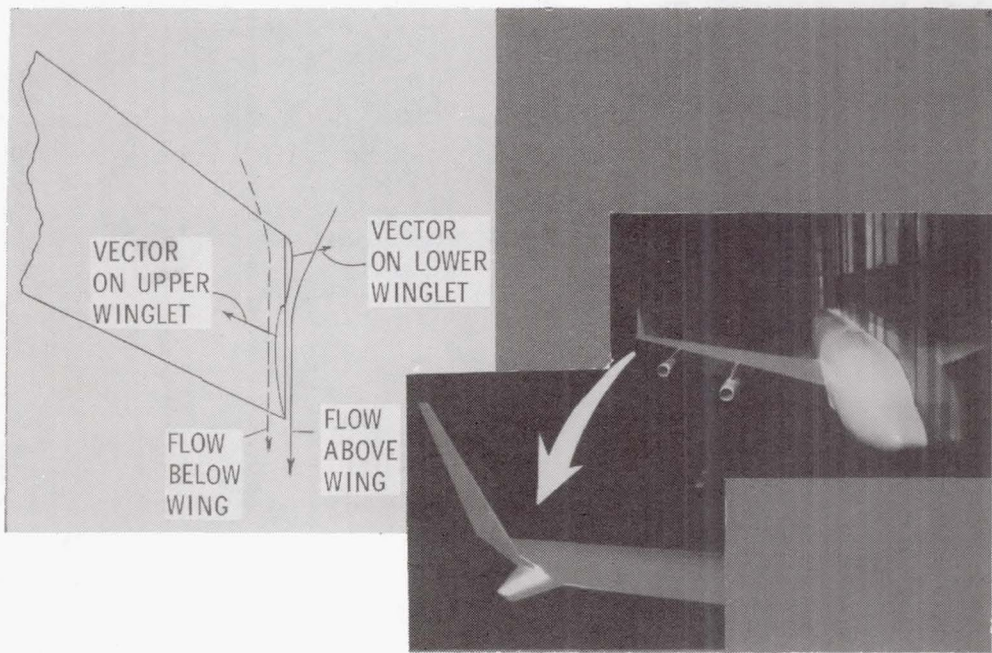


Figure 1.- Aerodynamic effect of winglets.

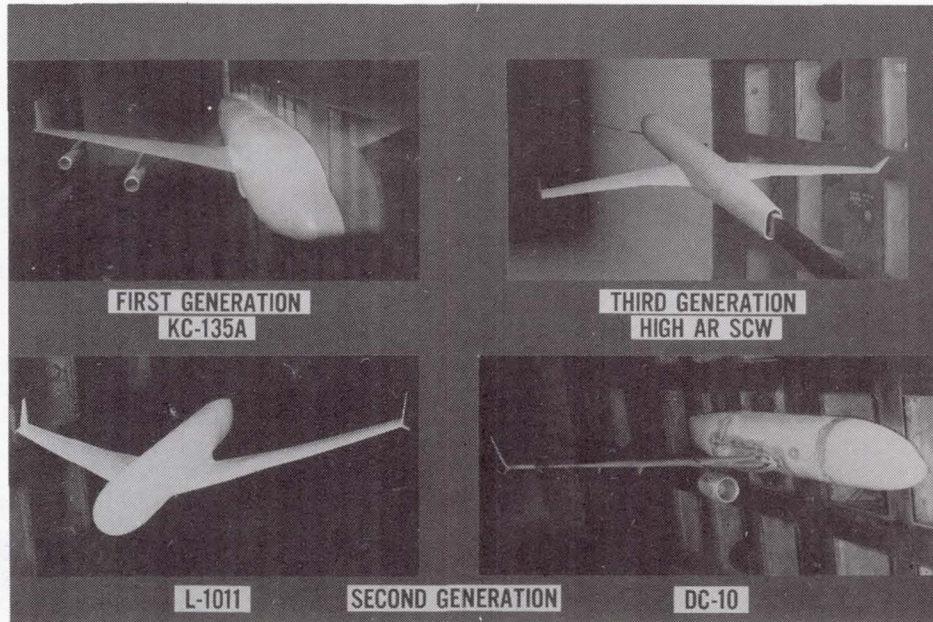


Figure 2.- Winglets on jet transport models.

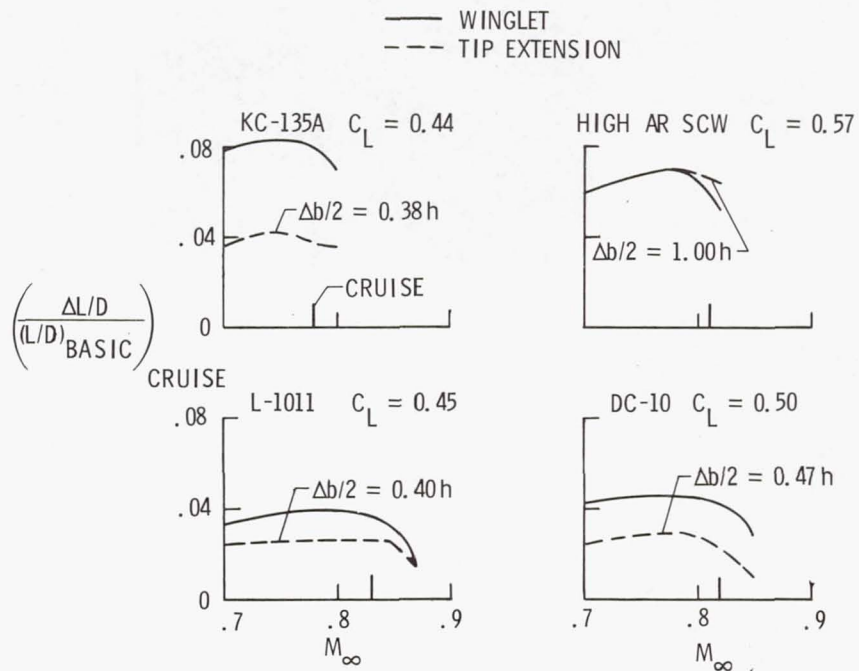


Figure 3.- Winglet and tip extension cruise performance.

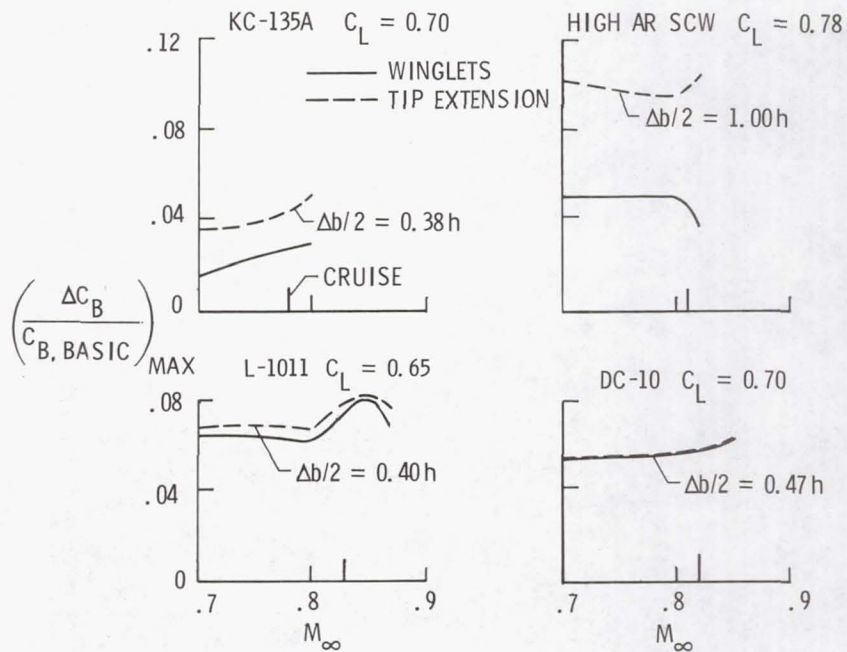


Figure 4.- Wing-root bending moments.

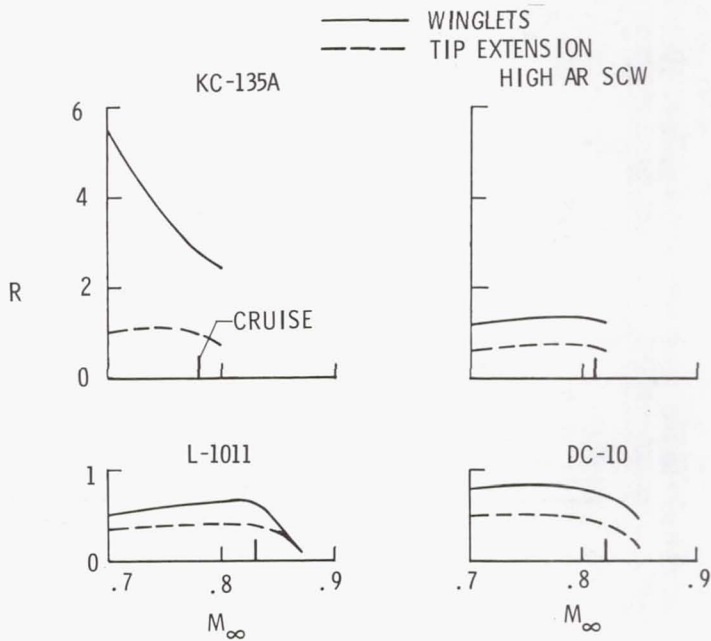


Figure 5.- Comparison of ratios of merit.

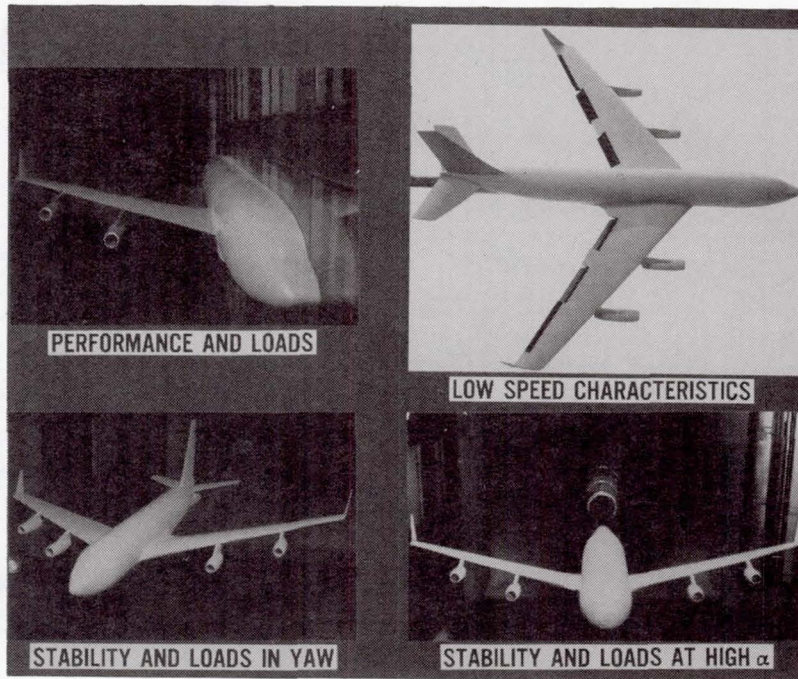


Figure 6.- Winglets on the KC-135A models.

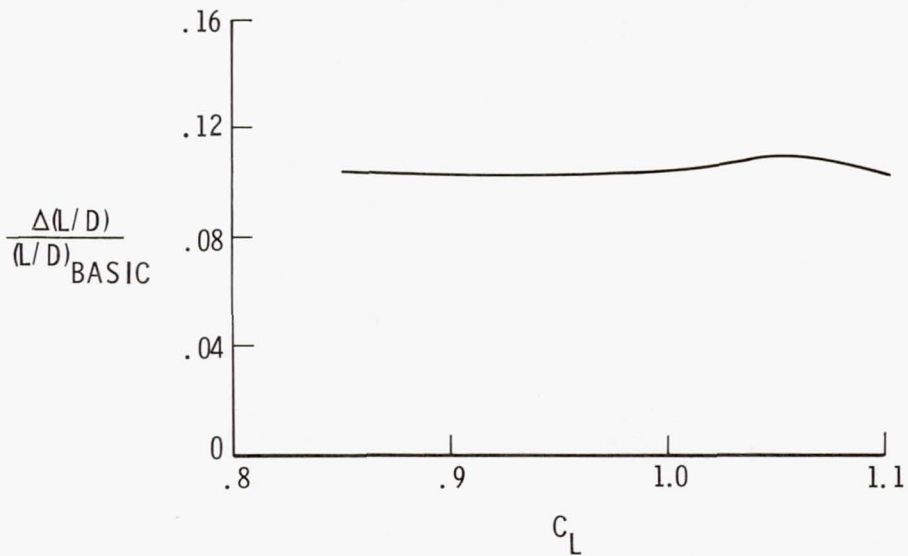


Figure 7.- Low-speed winglet performance. KC-135A semispan model with take-off flaps. $M_\infty = 0.30$.

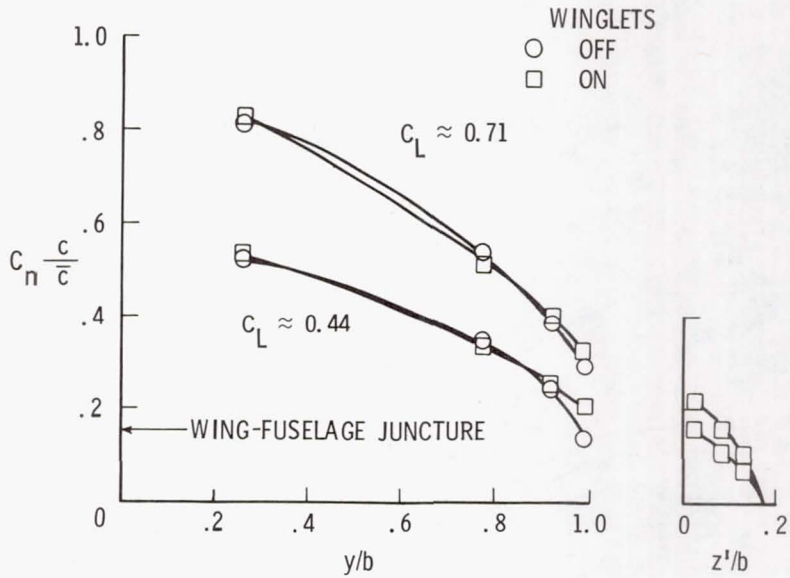


Figure 8.- Effect of winglets on spanwise load distributions. KC-135A semispan model. $M_\infty = 0.78$.

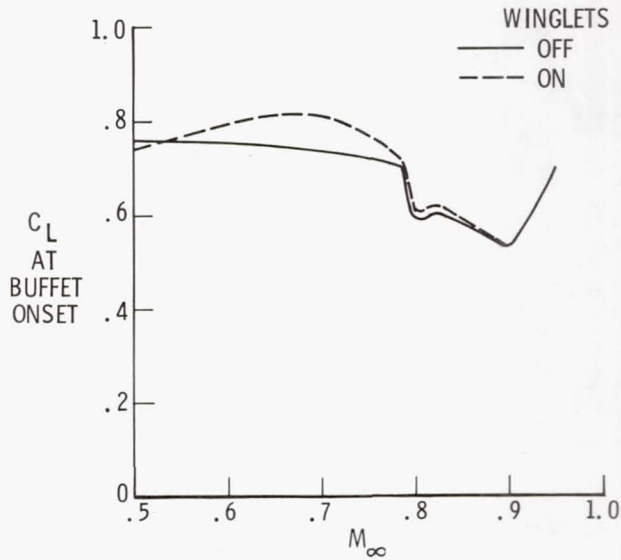
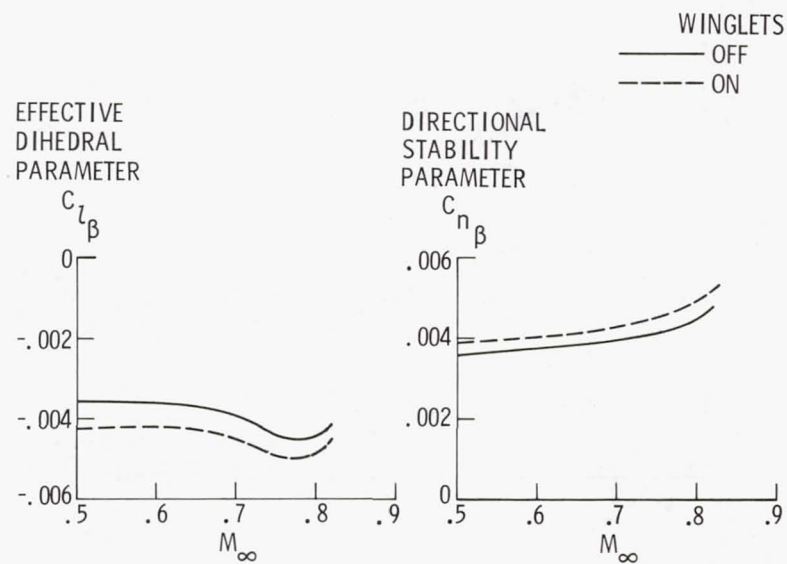
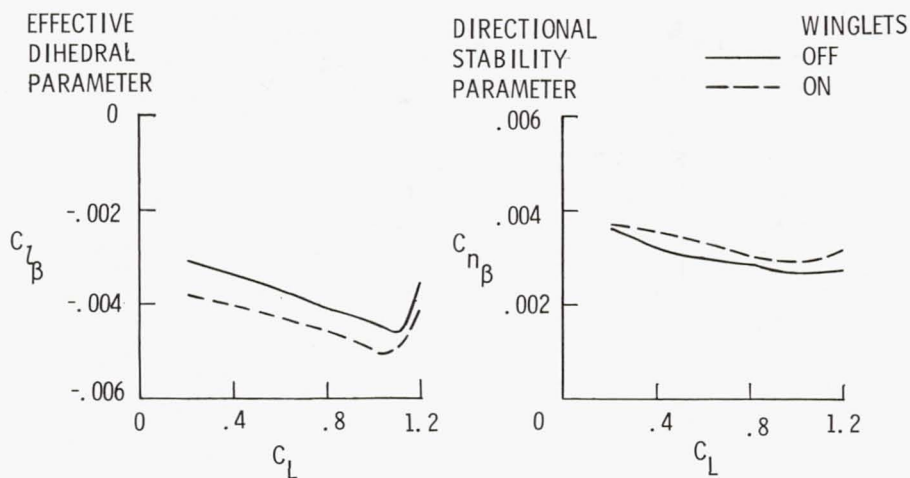


Figure 9.- Effect of winglets on high-speed buffet characteristics. KC-135A full-span tailless model.



(a) KC-135A full-span, high-speed model. $C_L = 0.44$; $\delta_h = 0^\circ$.



(b) KC-135A full-span, low-speed model. $M_\infty = 0.30$; $\delta_{a,L} = -10^\circ$; $\delta_{a,R} = 10^\circ$;
 $\delta_f = 30^\circ$; $\delta_h = -10^\circ$.

Figure 10.- Effect of winglets on lateral-directional stability.

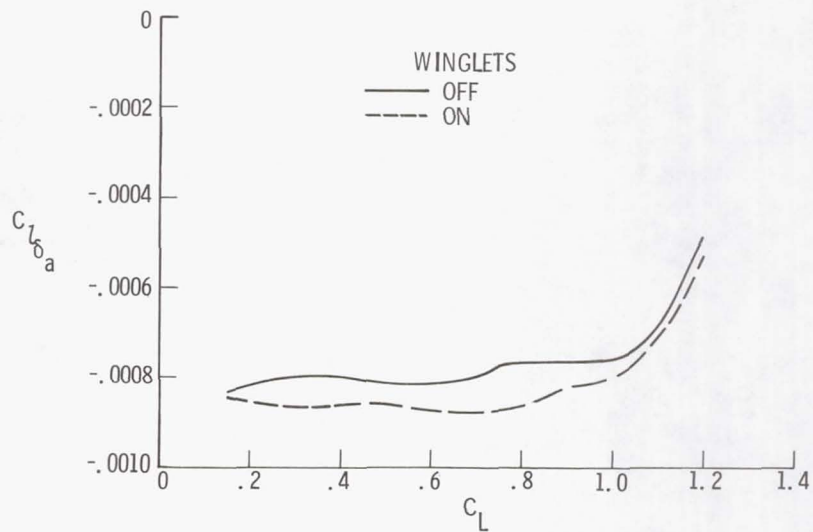


Figure 11.- Effect of winglets on aileron control effectiveness. KC-135A full-span, low-speed model. $M_\infty = 0.30$; $\beta = 0^\circ$; $\delta_f = 30^\circ$; $\delta_h = -10^\circ$.



Figure 12.- USAF KC-135A with NASA winglets.